Region-Specific DNA Damage by AT-Specific DNA-Reactive Drugs Is Predicted by Drug Binding Specificity[†,‡]

Jan M. Woynarowski,* Cheryl Napier, Alex V. Trevino, and Brenda Arnett

Cancer Therapy and Research Center, 14960 Omicron Drive, San Antonio, Texas 78245

Received March 30, 2000; Revised Manuscript Received May 25, 2000

ABSTRACT: Bizelesin and adozelesin are DNA-reactive antitumor drugs that alkylate adenines at the 3′ ends of their preferred binding sites [5′T(A/T)$_4$A3′and 5′(A/T)$_{3-4}$A3′, respectively]. We used these drugs to examine the determinants for region-specific damage of human genomic DNA. The distribution of bizelesin binding motifs in several regions analyzed "in silico" correlated well with the experimentally determined lesions in these regions assessed by quantitative polymerase chain reaction (QPCR) stop assay. In contrast to the typically low motif density, clusters of potential bizelesin binding sites were found in the matrix-associated regions (MAR domains) of the c-*myc* and apolipoprotein B (*apoB*) genes. Accordingly, lesions induced by bizelesin in these domains (2.13 and 7.06 lesions kbp^{-1} μM^{-1}, respectively) markedly exceeded lesions in bulk DNA (0.87 lesions kbp^{-1} μM^{-1}) or in regions with typically low motif density (e.g., 0.75 and 0.87 lesions kbp^{-1} μM^{-1} in a β-globin gene and c-*myc* origin of replication regions, respectively). Consistent with the more frequent, less localized adozelesin motif, actual lesions induced by adozelesin exceeded by severalfold lesions by bizelesin in four selected regions (within the c-*myc* and *HPRT* loci). Whereas adozelesin is likely to affect similar regions as bizelesin, adozelesin's more promiscuous binding probably compromises its relative specificity for such targets. In contrast, findings for bizelesin provide for the first time a proof of principle that a small molecular weight drug can preferentially damage specific regions in cellular DNA. Targeting of critical repetitive sequences, such as AT-rich MAR domains, which allow for clustering of drug binding motif, can be the paradigm for region specificity of small molecular weight agents.

DNA minor-groove binding agents are among the most DNA sequence-specific small molecular weight drugs. Various compounds of this class have been designed and studied for their potential as anticancer drugs, with the hope that their high sequence specificity will ultimately allow for selective targeting of specific cellular processes in tumor cells (for review see refs *1* and *2*). Several natural and synthetic minor-groove binding drugs exhibit a profound cytotoxic and antitumor in vivo activity, and some of these compounds are being evaluated clinically.

One class of AT-specific minor-groove binding drugs under clinical investigation (*3*) is the cyclopropylpyrroloindole (CPI)[1] family, which includes drugs such as adozelesin and bizelesin (Figure 1). In addition to a noncovalent interaction with the minor groove, these agents are capable

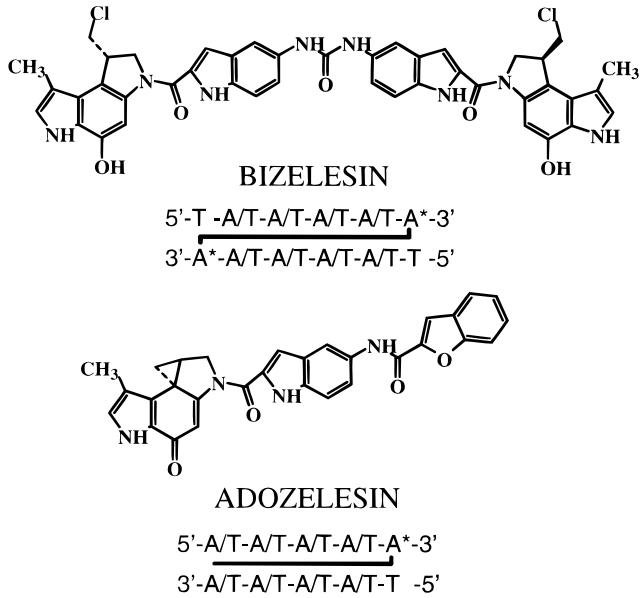

FIGURE 1: Structures and preferred DNA binding motifs of bizelesin and adozelesin. Both drugs bond covalently adenines at the 3′ ends of their binding sites (asterisks) via chloromethyl groups (bizelesin) and cyclopropyl group (adozelesin). The preferred binding motif for bizelesin corresponds to interstrand cross-link, although bizelesin can form also monoadducts, preferably with A(A/T)$_4$A* motifs. Adozelesin, with a single alkylating moiety, can form only monoadducts with DNA. In addition to the preferred motif shown, adozelesin tolerates G/C at the 5′ side of its binding motifs with the minimal requirement for (A/T)$_2$A*.

[†] This study was supported in part by a grant from the National Cancer Institute (CA71969).

[‡] A preliminary account from this study has been presented in part at Eighty-Eighth Annual Meeting of American Association for Cancer Research, April 1997, San Diego, Proceedings of the American Association Cancer Research Abstract 1535.

* To whom correspondence should be addressed at Cancer Therapy and Research Center, Institute for Drug Development, 14960 Omicron Dr., San Antonio, TX 78245-3217. Phone 210-677-3832; Fax 210-677-0058; e-mail: jmw1@saci.org.

[1] Abbreviations: ApoB, apolipoprotein B; CPI, cyclopropylpyrroloindole; HPRT, hypoxanthine phosphoribosyltransferase; HVR, hypervariable region; MAR, matrix-associated regions; ORI, origin of replication; QPCR, quantitative polymerase chain reaction; SV40, simian virus 40.

10.1021/bi000729k CCC: $19.00
Published on Web 07/18/2000

of covalent bonding to adenines at the 3′ ends of their binding sites. Adozelesin occupies 5 bp sites preferably consistent with the motif 5′(A/T)$_{3-4}$A3′and forms only monoadducts with DNA. Since the drug tolerates occasionally a G or C near the 5′ end of the binding site (*4*−*6*), the minimal consensus binding sequence of adozelesin is 5′(A/T)$_2$A3′. Bizelesin binding sites on DNA generally correspond to 6 bp motifs, mainly 5′T(A/T)$_4$A3′. With this binding motif, bizelesin forms two covalent bonds with the adenines at both 3′ ends (Figure 1), resulting in interstrand cross-links (*7*−*10*). Specific sites adducted by these drugs in cellular DNA are virtually identical to those in naked DNA (*5*, *9*, *10*), indicating that DNA sequence is their primary determinant. In addition to a remarkable sequence specificity of their DNA binding motifs, CPI analogues react only with DNA, which distinguishes them from typical DNA-reactive anticancer drugs that form a spectrum of lesions with various cellular macromolecules.

CPI analogues are extremely potent inhibitors of genomic replication, acting at the level of new replicon initiation (*11*). Intriguingly, only a single bizelesin adduct per approximately 10 genomic replicons is necessary for a nearly complete inhibition of replicon initiation. Our previous studies demonstrated also that matrix-associated region (MAR) and origin of replication (ORI) of intracellular SV40 DNA are among the preferred targets for CPI drugs (*9*, *12*, *13*). Genomic MARs, which are crucial for cellular DNA replication (*14*, *15*), are often AT-rich (*16*, *17*). Hence, we speculated that targeting AT-rich replication-related genomic regions could be an important factor in the high antiproliferative and antireplicative potency of CPI drugs. Also, it was possible that the consistently observed greater cytotoxicity of bizelesin than adozelesin (*18*−*20*) could be related to the more specific DNA lesions. However, except for our recent study with an unrelated AT-specific minor-groove binding drug, tallimustine (*21*), region specificity of DNA-damaging AT-specific drugs remains unexplored.

This study characterized the ability of bizelesin to generate region-specific lesions in selected domains, including replication-related regions, and in bulk genomic DNA. The results show that bizelesin preferentially damages AT-rich domains such as AT-rich MAR regions. The less stringent binding motif of adozelesin results in more frequent and less localized lesions than bizelesin adducts, suggesting that even relatively small differences in drug binding motifs can influence as well as predict drug propensity for specific regions.

MATERIALS AND METHODS

Chemicals. Bizelesin (synonym U77779) and adozelesin (synonym U-73975) were generously provided Drs. Patrick McGovren and Robert Kelly at the Upjohn & Pharmacia Co. (Kalamazoo, MI) and their stock solutions were made in *N*,*N*-dimethylacetamide. Stock solutions were stored at −20 °C protected from light. Culture medium (Joklik's MEM) was from Gibco-BRL, (Gaithersburg, MD). [^{14}C]Thymidine (59.7 mCi/mmol) was from Dupont NEN (Boston, MA). Agarose was from FMC (Rockland ME). All other chemicals were reagent-grade.

Cell Culture and Cytotoxic Activity. Human CEM leukemia cells (from Dr. William T. Beck, University of Illinois, Chicago) were cultured in suspension in Joklik's medium containing 10% fetal bovine serum (*21*, *22*).

Drug cytotoxic activities against CEM cells were assayed on the basis of cell counts in an electronic counter after a 48 h incubation of 0.2×10^3 cells/mL. Cell counts before drug treatment (N_0) and at the end of a 48 h incubation in drug-treated and control samples (N_{tr} and N_{con}, respectively) were determined. These values were used to calculate cell growth relative to control (RG) as a ratio of $(N_{tr} - N_0)/(N_{con} - N_0)$ and drug concentration inhibiting relative cell growth by 50% (GI_{50}) (*23*).

Quantitative Polymerase Chain Reaction Stop Assay. QPCR on DNA from drug-treated cells was performed essentially as described previously (*21*, *24*, *25*). CEM cells were prelabeled with [^{14}C]thymidine and treated with drugs for 4 h followed by DNA extraction and purification with either PureGene (Gentra Systems, Minneapolis, MN) or Qiagen kits. The amounts of template DNA used in PCR reactions were expressed as cell equivalents based on ^{14}C radioactivity of DNA preparations (*21*, *25*). PCR reactions were carried out in replicates at 2−3 different cell equivalent levels. The PCR Core Reagents kit (Perkin-Elmer) was usually used to set PCR reactions, which consisted of 1× buffer II, 1.5−2.5 mM $MgCl_2$, 0.2 mM each dNTP, except for dGTP (0.05 mM), 1 unit of Taq polymerase, and 0.04 μCi/reaction [^{32}P]dGTP (NEN) and respective primers at 0.2−0.4 μM, unless noted otherwise. For each primer system, the amounts of template DNA and the number of cycles were chosen so as to ensure the linearity of the signal as a function of the amount of undamaged template.

Primer systems and cycling conditions for the c-*myc* PCR systems—a 743-bp region (positions 11−754), which includes the c-*myc* ORI domain, and a 947-bp region (positions 7114−8060), which includes the c-*myc* MAR domain, were used as described (*21*). A 2.7 kbp region in the hypoxanthine phosphoribosyltransferase (HPRT 2.7) locus spanning the positions 14578−17287 was amplified by use of the primer system of Oshita et al. (*26*, *27*) and conditions described previously (*25*). A 723 bp domain of the *HPRT* gene spanning the positions 5560−6282 and containing a region with a homology to yeast autonomously replicating sequences (HPRT ARS) (*28*) was amplified with 5-TAACAGCTTTATCCCTCAGAA-3′ and 5′-GTGGGTCCAAACAAGAC-3′ as upper and lower primer, respectively. HPRT ARS PCR reactions carried out with initial denaturation at 95 °C for 30 s followed by 26 cycles of 94 °C for 15 s, 50 °C for 20 s, and 72 °C for 25 s and a final 180 s at 72 °C. Primer systems of Daoud et al. (*29*) were used for β-globin and mitochondrial DNA (mito-DNA). QPCR conditions for these systems have been described previously (*25*).

Primer system for apolipoprotein B hypervariable region (HVR)/MAR domain (*ApoB* MAR) used 5′-ATTGAAAGACAGTGAAACGAGG-3′ and 5′-TATTGCCATGAAGCCCCT-3′ as the upper and lower primers, respectively. The primers were designed to anneal outside of the hypervariable repetitive region, spanning the positions 14658−15655 [as per sequence numbering of Levy-Wilson and Fortier (*30*)] to yield a product of nominal length of 998 bp. The actual PCR products exhibited showed two bands of ∼1.0 and 1.2 kbp reflecting the well-known length polymorphism of this locus (*31*). Both bands represent the *apoB* HVR/MAR sequences, as confirmed on the basis of their hybridization

to a probe (5′-AAAATATGGTAATTATAAACATTTTAATTAT-3′) designed for the repetitive motif of the hypervariable region (data not shown). The ApoB PCR was carried out with initial denaturation at 95 °C for 30−100 s followed by 25 cycles of 95 °C for 30 s, 53 °C for 15 s, and 60 °C for 60 s and a final 300 s at 72 °C.

Alu PCR used TC65 primer at 1 μM as described by Tsongalis et al. (*32*) and cycling conditions: initial denaturation at 95 °C for 30 s followed by 27 cycles of 94 °C for 30 s, 55 °C for 30 s, and 72 °C for 30 s and a final 180 s at 72 °C.

Following amplification, samples were electrophoresed in 1% agarose and autoradiographed. Signal intensities were quantitated in a Molecular Dynamics densitometer. In some experiments with c-*myc* regions, the amplified PCR products were immobilized on nylon membranes in a dot blot apparatus followed by the determination of radioactivity of the dots in a Packard Top Count scintillation counter. Since both quantitation variants gave virtually identical results, data from both variants were combined in subsequent data processing.

The results were normalized to the signal intensity in control samples and averaged for replicates and different levels of template DNA to yield the remaining amplification (F_a) values (*21*). Relative amplification data were further converted to lesion frequency by use of a Poisson distribution formula (eq 1) and expressed as lesions kbp^{-1} (μM drug)$^{-1}$ (*12*, *21*, *25*):

$$f = \frac{-\ln F_a}{L} \tag{1}$$

where f is the number of drug-induced lesions per base pair, F_a represents the fraction of remaining amplification (relative to control) in drug-treated samples, and L is the length of target DNA region in bp. In some cases where F_a exceeded 1, f values were forced to 0.

Analysis of DNA Sequences for Drug Binding Motifs. The numbers and positions of drug binding motifs in each region were obtained by analyzing DNA sequences for these regions with a tool in Oligo (NBI) program that was originally designed for restriction site searches. The motif input data included 5′-T(A/T)$_4$A-3′ for bizelesin (*4*, *9*, *10*) and 5′-(A/T)$_4$A-3′ for adozelesin (*4*, *5*). The number of bizelesin motifs/kbp of bulk DNA was estimated from the probability of random occurrence as outlined in ref *33*, with the value of 60% A/T.

Total Adducts in Bulk Cellular DNA of Intact Cells. Covalent adducts of bizelesin and adozelesin in genomic DNA of intact CEM cells were quantitated on the basis of induction of heat-labile sites as described previously for CC-1065, adozelesin, and bizelesin (*9*, *18*, *34*), except that only [^{14}C]thymidine labeling and external controls were used (*21*). Briefly, [^{14}C]thymidine-prelabeled CEM cells (0.5×10^5 cells/mL) were incubated with drugs as indicated, washed with cold PBS and lysed in 1% Sarkosyl, 1 M NaCl, and 10 mM EDTA, pH 8.6. Cell lysates were heated for 15 min at 95 °C and their aliquots (150 μL) were loaded onto 5−20% alkaline sucrose gradients (in 2 mM EDTA, 300 mM NaOH, and 700 mM NaCl) composed as described previously (*21*). After 1 h lysis at 20 °C, gradients were centrifuged at 17 000 rpm (36500*g*) for 19 h in an SW40Ti rotor (Beckman-Coulter,) followed by the fractionation and processing of gradient fractions as described (*9*, *34*).

Frequencies of heat-labile sites (breaks) in genomic DNA were calculated as described previously (*9*, *34*):

$$f = \frac{[(MW_n)_A/(MW_n)_B] - 1}{(MW_n)_A/640} \tag{2}$$

where f is the number of breaks per base pair and $(MW_n)_A$ and $(MW_n)_B$ are number-average molecular weights of DNA peaks from control and drug-treated cells, respectively. The value 640 represents the average molecular weight of one DNA base pair. The number-average molecular weight was determined from:

$$(MW_n) = \frac{\sum \%R_i}{\sum \%R_i/MW_i} \tag{3}$$

where $\%R_i$ is percent of recovered radioactivity for each fraction of a given peak and MW_i is the molecular weight of the corresponding fraction.

RESULTS

Selection of Regions for Quantitative PCR Stop Assay To Compare Region Specificity of Bizelesin and Adozelesin. The QPCR stop assay is used to monitor the formation of lesions in specific regions of cellular DNA based on the impeded amplification of drug-adducted template (*21*, *25*). To assess region-specific effects of the studied drugs on a reasonably representative sample of possible target sequences, we selected regions of the c-*myc* and hypoxanthine phosphoribosyltransferase (*HPRT*) genes (*35*), as examples of protooncogenic and nononcogenic ubiquitously expressed gene loci, respectively. The complete structures and various functional elements of these two relatively small genes are known (*36*−*40*). In the cell line used in these studies, human acute lymphoblastic leukemic CEM, the c-*myc* gene is known to be overexpressed (i.e., activated) compared to normal lymphocytes and normal T-cells (*41*).

The potent effects of CPI drugs on replication (*11*) suggested the possibility that replication-related regions may be among potential drug targets. Thus, regions selected in the c-*myc* locus were replication-related domains MAR and ORI (*37*−*40*) (see Figure 2A). In addition, one of the two HPRT systems selected included an ARS element (*28*), a domain homologous to replication-related yeast autonomously replicating sequences. The selected regions covered a broad range of AT content: 50.8% and 63.5% for the c-*myc* ORI and MAR, respectively, and 60.5% and 63.8% for the HPRT ARS and HPRT2.7, respectively.

Less Specific Drug, Adozelesin, Induces More Lesions Than the More Specific Drug, Bizelesin. The map of the c-*myc* gene depicts the localization of the MAR and ORI domains and the positions of PCR primers that we developed for these target regions (Figure 2A). The density of potential binding sites for both bizelesin and adozelesin is rather low in the entire c-*myc* locus (Figure 2A). Still, the less stringent binding motif of adozelesin is clearly more frequent than the bizelesin motif. It is also noticeable that the motif distribution is nonrandom with fairly long stretches devoid of the preferred binding sites.

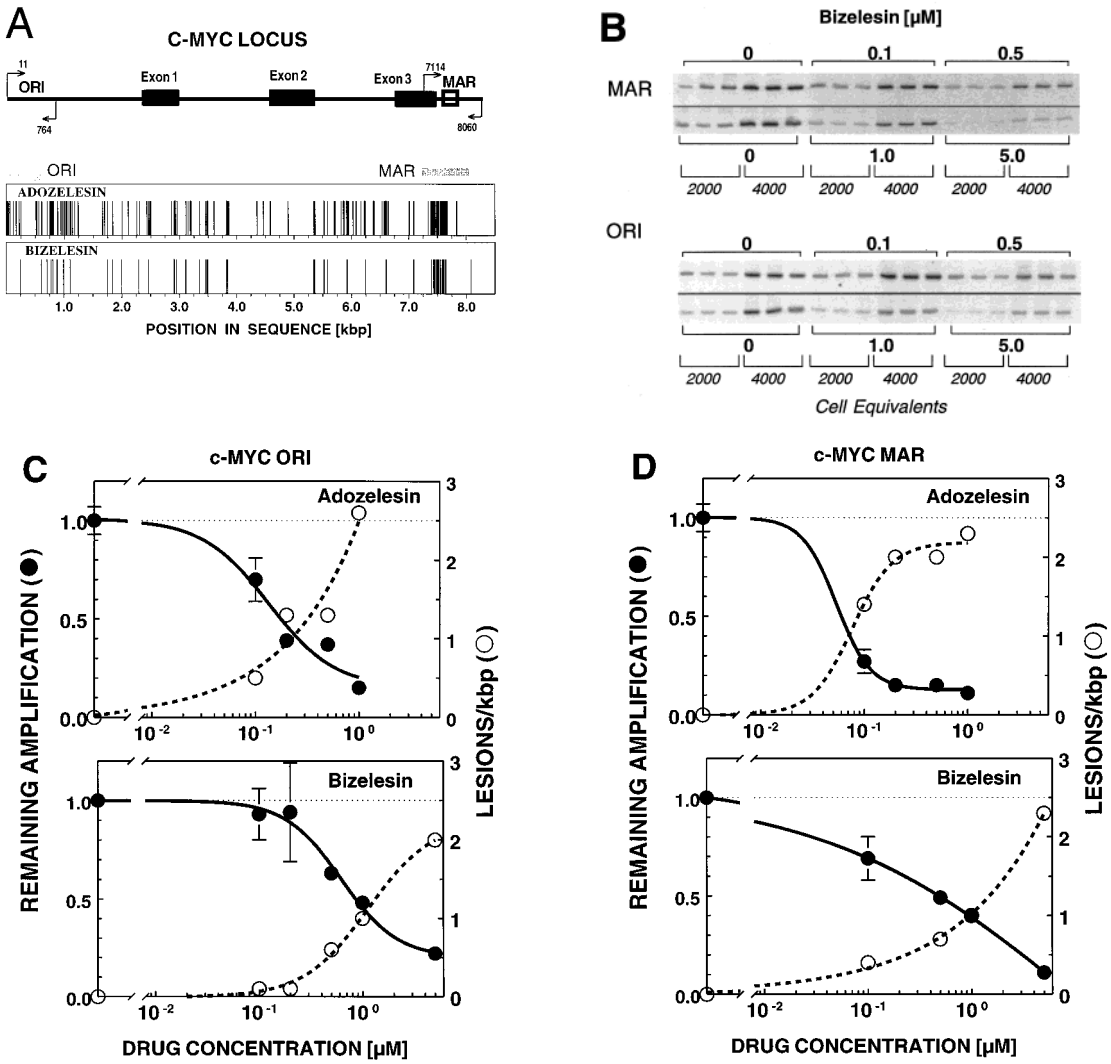

FIGURE 2: Lesions by induced in CEM cells by bizelesin and adozelesin in two regions of a protooncogenic locus (ORI and MAR regions of the c-*myc* gene). (A) Map of the c-*myc* gene (top) and the distribution of $(A/T)_4A$ and $T(A/T)_4A$ as potential adozelesin and bizelesin binding motifs, respectively (bottom). The arrows on the map and horizontal bars in the motif distribution panels show the regions amplified in QPCR stop assay experiments (c-*myc* ORI and c-*myc* MAR, cf. panels B and C). The distribution of drug binding motifs has been obtained by the analysis of c-*myc* sequence with the Oligo program. (B) Representative agarose electrophoresis of amplified c-*myc* ORI and c-*myc* MAR with DNA from control cells and cells incubated for 4 h at 37 °C with the indicated bizelesin concentrations. Different amounts of template DNA are indicated as cell equivalents. (C) Quantitation of lesions in c-*myc* ORI region. (D) Quantitation of lesions in c-*myc* MAR region. Remaining amplification in panels C and D (●, left axes) represents averaged values, normalized to the amplification of control DNA, from 3−7 and 2−3 independent experiments (±SE, where they exceeded marker size) for bizelesin and adozelesin, respectively. The frequencies of drug-induced region-specific lesions (○, right axes) in panels C and D were estimated from a Poisson distribution formula as described under Materials and Methods.

The results of the QPCR stop assay demonstrate that both bizelesin and adozelesin form lesions in replication-related regions of the c-*myc* oncogene. Examples of agarose electrophoresis (Figure 2B) illustrate the gradual, concentration-dependent elimination of the PCR signal in DNA from drug-treated cells. Quantitation of these effects and the estimated lesion frequencies are given in panels C and D of Figure 2. Bizelesin at 0.1 μM has a measurable effect in the MAR region. The ORI region, however, is significantly affected by bizelesin only at 0.5 μM and higher concentration. For adozelesin, the definite decrease of the PCR signal is observed at 0.1 μM adozelesin in both ORI and MAR, although the inhibition is also more profound in the MAR domain. Apart from the plateau of adozelesin effects at 0.5−1 μM drug, the actual lesion frequencies demonstrate clearly that the more specific bizelesin induces fewer lesions than the less specific adozelesin.

The lower propensity of both drugs for the c-*myc* ORI (compared to the c-*myc* MAR), while not dramatic, has been consistently observed, especially for bizelesin. This difference parallels the lower abundance of drug binding motifs in the ORI sequences and the presence of an AT island with clusters of binding sites for both drugs in the MAR sequences. However, the PCR system for the MAR region includes a substantial length of sequences that, while flanking the AT island in the center, are nearly devoid of the preferred drug binding sites. Thus, lesion frequency equalized over the entire PCR amplicon could markedly underestimate the preference for the central cluster of drug binding sites.

Higher frequency of adozelesin than bizelesin lesions was corroborated by use of PCR systems for two regions of a nononcogenic HPRT gene, referred to as HPRT ARS and HPRT 2.7. Sequence analysis for drug binding motifs confirmed that both regions contain markedly more sites for

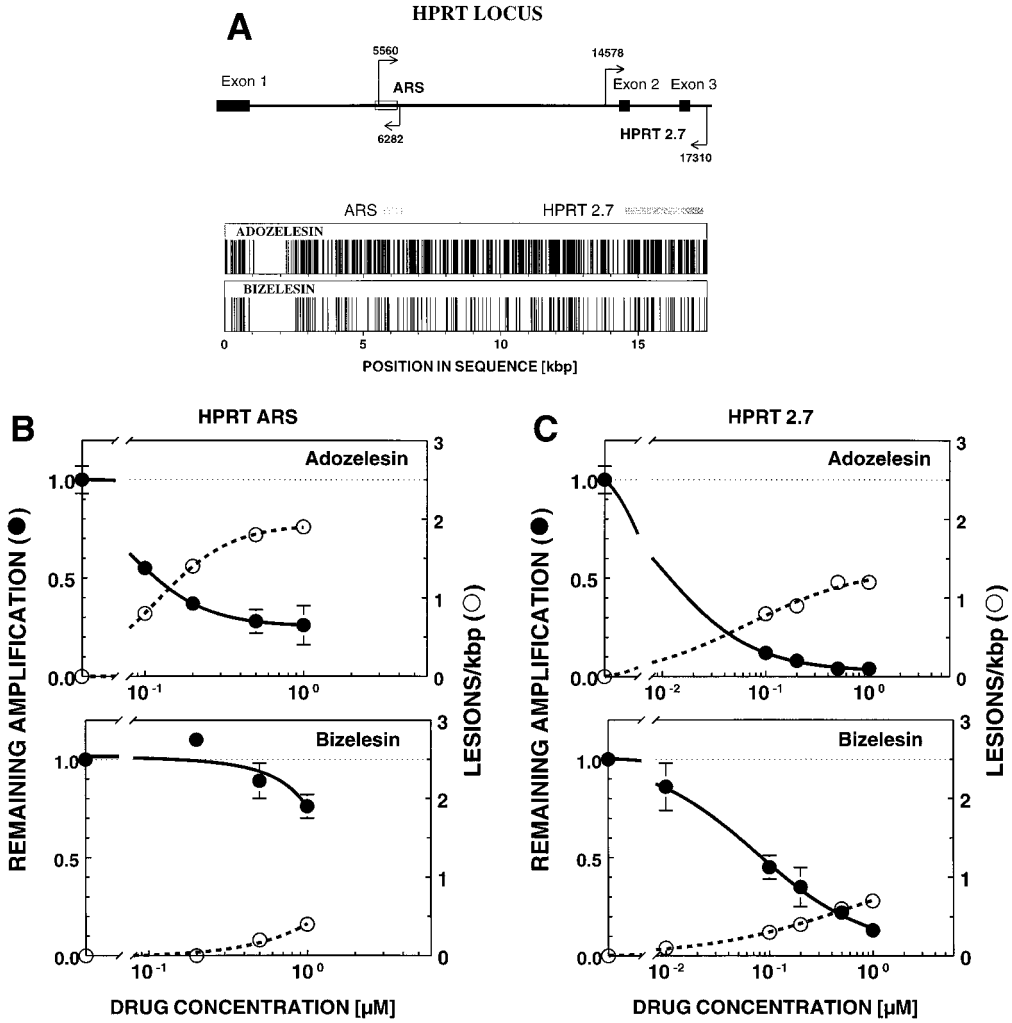

FIGURE 3: Lesions by induced in CEM cells by bizelesin and adozelesin in two regions of a nononcogenic locus (*HPRT* gene). (A) Partial map of *HPRT* gene (top) and the distribution of $(A/T)_4A$ and $T(A/T)_4A$ as potential adozelesin and bizelesin binding motifs, respectively (bottom). The arrows and horizontal bars show the regions amplified in QPCR stop assay experiments (HPRT ARS and HPRT 2.7). (B) Drug lesions in HPRT-ARS region. (C) Drug lesions in HPRT 2.7 region. Remaining amplification (●, left axes) represents averaged values, normalized to amplification of control DNA, from 2−6 independent experiments (±SE, where they exceeded marker size). The frequencies of drug-induced region-specific lesions (○, right axes) were estimated from a Poisson distribution formula.

adozelesin than for bizelesin. In particular, HPRT ARS was found to be very poor in potential bizelesin binding sites (Figure 3A). Accordingly, bizelesin induced approximately 2-fold fewer lesions in the ARS region than in the HPRT 2.7 region (Figure 3B,C). At the same time, as with the c-*myc* regions, adozelesin was markedly more efficient than equimolar bizelesin in reducing the amplification signal in both systems. Corresponding estimates of lesion frequency clearly indicate that adozelesin formed 2−3-fold and 5−9-fold more lesions in HPRT 2.7 and HPRT ARS, respectively.

Bizelesin Preferentially Damages AT-Rich MAR Regions over Non-MAR Domains. The c-*myc* locus data suggested that certain AT-rich domains may contain clusters of potential bizelesin binding sites and, therefore, can be more vulnerable to drug-induced DNA lesions. Thus, further experiments examined bizelesin effects in a well-characterized AT-rich MAR region of apolipoprotein B (ApoB, Figure 4A). Noteworthily, ApoB MAR coincides with a hypervariable region, a locus that is known for its extensive length polymorphism reflecting a variable number of tandem repeat sequences (*31*). Sequence analysis shows that ApoB MAR contains a cluster of many preferred bizelesin binding motifs (Figure 4A). The ApoB PCR system designed by us included this AT MAR and relatively short flanking sequences with a PCR product corresponding to nearly 80% AT content.

The amplified signal for the ApoB PCR system showed two main bands of ∼1.0 and 1.2 kbp (Figure 4C, top), which are consistent with two alleles containing approximately 37 and 49 repeat units of the 14−16 bp repetitive element (*31*). Since bizelesin inhibited to the same extent the amplification of both alleles, both bands were quantitated together and their average length (1100 bp) was used in the estimations of lesion frequencies. The agarose electrophoresis (Figure 4C) and its quantitation (Figure 4D) demonstrate a profound inhibitory effect of bizelesin treatment on the amplification of ApoB MAR with DNA from drug-treated cells. A detectable inhibition was seen at 0.01 μM drug, whereas 0.5 μM bizelesin produced a nearly complete elimination of the signal.

The results with AT-rich ApoB MAR domain are in striking contrast to the insensitivity of a non-MAR AT-poor domain in the β-globin gene (Figure 4B−D). Sequence analysis shows that the β-globin PCR system reflects only 46.8% AT and does not contain any preferred bizelesin

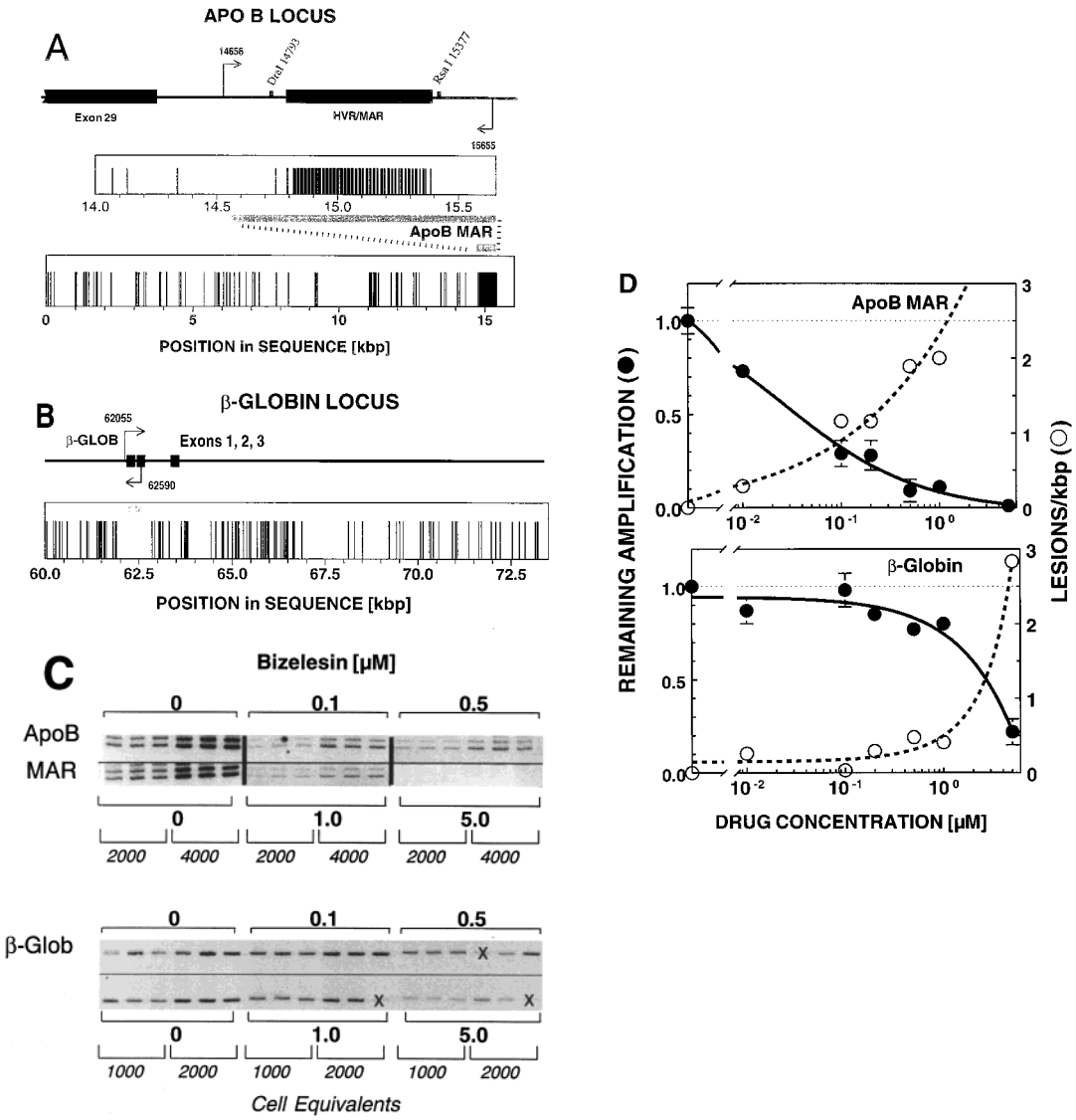

FIGURE 4: Differential lesion induction by bizelesin in an AT-rich MAR region (in *apoB* gene) versus an AT-poor non-MAR region (in *β*-globin gene) in drug-treated CEM cells. (A) Partial map of the 3′ end of *apoB* gene (top) and the distribution of $T(A/T)_4A$ as potential bizelesin binding motifs (bottom). HVR/MAR indicates the hypervariable domain, which coincides with MAR domain and is flanked with *Dra*I and *Rsa*I sites (*30*). Note that HVR/MAR region closely coincides with the cluster of potential bizelesin binding sites. The arrows and horizontal bars show the region amplified in QPCR stop assay experiments denoted ApoB MAR. (B) Partial map of *β*-globin gene (top) and the distribution of $T(A/T)_4A$ as potential bizelesin binding motifs (bottom). The arrows and horizontal bars show the region amplified in QPCR stop assay experiments denoted *β*-globin non-MAR. Note that this region does not contain any preferred bizelesin binding sites. (C) Representative agarose electrophoresis of amplified ApoB MAR with DNA from control cells and cells incubated for 4 h with the indicated bizelesin concentrations. Doublet bands correspond to different alleles of a hypervariable region, which coincides with *apoB* MAR. Different amounts of input template DNA are indicated as cell equivalents. An X denotes a replicate lane rejected as an outlier. (D) Quantitation of bizelesin lesions in ApoB MAR region and in *β*-globin non-MAR regions. Remaining amplification (●, left axes) represents averaged values, normalized to the amplification of control DNA, from 2−7 independent experiments (±SE, where they exceeded marker size). The frequencies of drug-induced region-specific lesions (○, right axes) were estimated from a Poisson distribution formula as described under Materials and Methods. For details see Materials and Methods.

binding motif (Figure 4B). This does not necessarily mean that bizelesin should not bind in this domain, since, as mentioned previously, the preferred motif is not the only sequence that bizelesin can react with. Still, the QPCR gel and the quantitation of drug effects (Figure 4C,D) indicates a marginal effect on the amplification of the *β*-globin region up to 1 *μ*M bizelesin, i.e., more than needed to nearly completely wipe out the signal in the ApoB MAR system. Only at the highest drug level examined (5 *μ*M) was a significant level of inhibition observed, probably reflecting drug binding to less preferred sites.

Differential Inhibition of Alu PCR Products Corroborates Region-Specific DNA Damage by Bizelesin. To further evaluate bizelesin-induced damage to various regions of cellular DNA, we examined drug effects by use of Alu PCR. Capitalizing on the repetitive nature of Alu sequences, Alu PCR utilizes a single primer to amplify non-Alu domains framed by copies of Alu repeats on the complementary strands (*32*). Alu PCR generates multiple products differing broadly in their sizes in a single PCR reaction (*32*) (Figure 5). Alu repeats per se are not a target for bizelesin, as various Alu subfamilies (*42*) tend to contain very few potential bizelesin binding sites (data not shown). However, Alu repeats are frequent in the vicinity of MAR domains (*32*), which often include AT islands (*43*, *44*), i.e., domains with clusters of potential bizelesin binding sites.

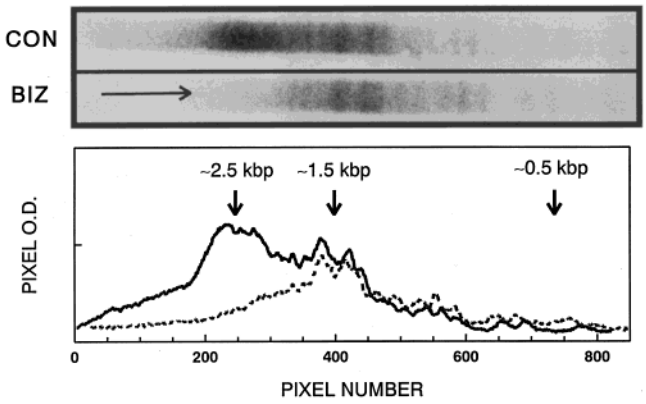

FIGURE 5: Inhibition of Alu PCR products in DNA from bizelesin-treated CEM cells. Alu PCR determinations were carried out as described under Materials and Methods with a single primer (TC65) to amplify a range of products flanked by Alu repeats. The top panel shows representative lanes of agarose gel for reactions with 5 ng of DNA from control and bizelesin-treated cells. Horizontal arrow indicates the direction of electrophoretic migration. The densitometric scans of these lanes are shown in the bottom panel.

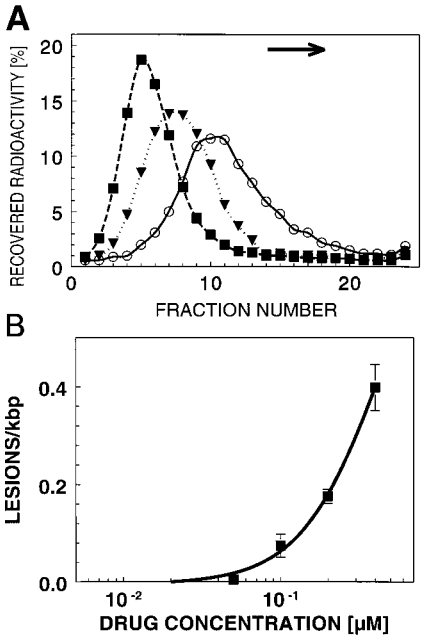

FIGURE 6: Bizelesin-induced damage to bulk genomic DNA of CEM cells monitored as thermally inducible breaks. (A) Representative alkaline sucrose gradient sedimentation profiles of [^{14}C]-thymidine-labeled DNA from CEM cells treated for 4 h with bizelesin at 0 (○), 0.2 (▼), and 0.4 μM (■) and processed as described under Materials and Methods. Cell lysates were heated for 15 min at 90 °C prior to loading on the gradients to convert drug adducts to strand breaks. Sedimentation was from left to right (arrow). (B) Quantitation of adduct frequency in genomic DNA based on thermally induced strand breaks monitored by sedimentation analysis such as in panel A (see Materials and Methods for details). Average values (±SE) from five independent experiments are shown.

Consistent with the effects in the QPCR systems, bizelesin treatment of CEM cells impedes also the amplification of Alu PCR products (Figure 5). At 0.2 μM drug, the overall signal summed up for all the products amounted to ~55% of the control. However, the inhibition was not uniform; the signal for the products greater than 1.5−2 kbp was nearly completely eliminated, whereas other bands for smaller products were only marginally affected. The identity of the bands whose amplification is severely inhibited remains unknown, and these results need to be regarded as preliminary. However, considering the aforementioned localization of Alu repeats near MAR sequences, it is highly likely that at least some of the strongly inhibited regions correspond to AT-rich MAR domains, corroborating QPCR data in specific regions.

Bizelesin Lesions in Bulk DNA and in Mitochondrial DNA. To put the results of region-specific lesions in the perspective of damage induced by bizelesin to the entire cellular DNA in CEM cells, we analyzed bizelesin lesions in bulk DNA. These measurements were based on thermal conversion of drug adducts to strand breaks, which in turn were analyzed by DNA sedimentation in alkaline sucrose gradients (*9*, *18*, *21*, *34*). The thermally induced strand breaks result in a decreased rate of DNA sedimentation that is dependent on drug concentration (Figure 6A). On the basis of the shifts in the sedimentation profiles, the frequency of drug-induced lesions can be estimated (Figure 6B). Bizelesin lesions in bulk DNA are clearly detectable at 0.1 μM drug and continue to increase, without reaching saturation, up to the highest level examined (0.4 μM), which produced an estimated ~0.4 lesion/kbp. Similar bizelesin reactivity was observed previously with BSC-1 cells (*9*).

Lesions in bulk DNA reflect mainly the nuclear DNA. For some drugs, however, a controversy exists as to whether nuclear or mitochondrial DNA is the main target (ref *25* and references therein). Therefore, we additionally analyzed bizelesin effects in a QPCR system designed for a region of mitochondrial DNA. This region contained some preferred bizelesin binding sites and had a higher AT content (~56%) than the β-globin system. Still, the inhibition of signal amplification and the estimated lesion frequency were comparably low (Figure 7A). The data for bizelesin lesions in bulk (i.e., mainly nuclear) DNA, mitochondrial DNA, and a preferred AT-rich island (ApoB MAR) are replotted on the same scale in Figure 7B. Given the very different methods, lesion frequencies in bulk and mitochondrial DNA are fairly close, suggesting that mitochondrial DNA is not preferentially affected over nuclear DNA. By contrast, this comparison clearly illustrates the gap between the average damage to genomic DNA and the profound preference for the AT-island MAR domain.

Predicted versus Actual Bizelesin Lesions: Correlation between Region-Specific DNA Damage and Motif Density. To further examine whether sequence specificity indeed predicts region specificity, bizelesin-induced damage to specific regions (normalized per kilobase pair/micromolar drug) was plotted against the number of drug binding motifs $T(A/T)_4A$ in the analyzed PCR products, which were also normalized for 1 kbp length (motif density). Drug-induced lesions in bulk DNA were included in the analysis. The results of this analysis show that the actual vulnerability of individual regions is positively correlated ($r = 0.963$) with the regional density of $T(A/T)_4A$ binding motif (Figure 8, top). Moreover, the actual lesion frequencies fall to very low levels for low densities of the $T(A/T)_4A$ motif. At the relatively high bizelesin concentrations needed for QPCR determination, some bizelesin molecules bind the monoadduct sites such as $(A/T)_5A$ (*12*). Therefore, another analysis included this monoadduct motif in addition to the cross-linking motif. The resulting correlation was similar, although

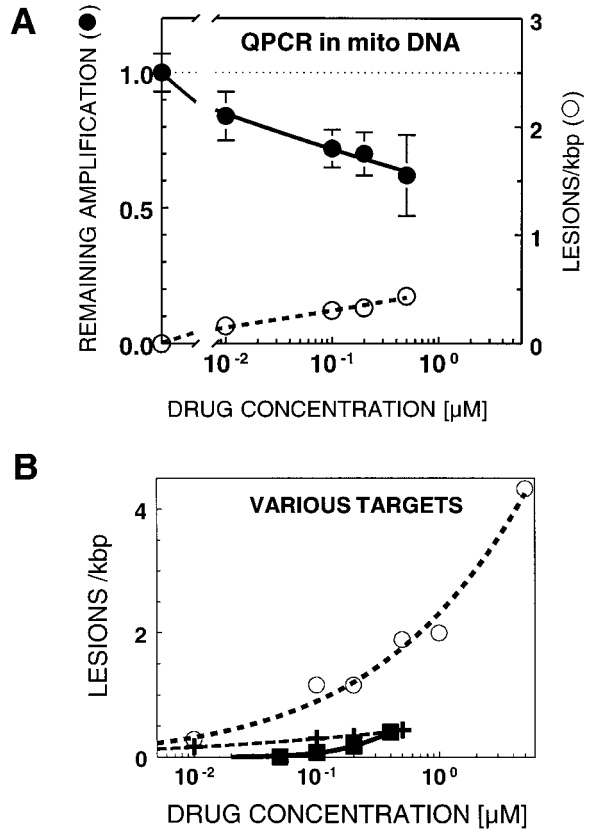

FIGURE 7: Ability of bizelesin to damage mitochondrial DNA versus bulk- and region-specific damage to nuclear DNA. (A) QPCR stop assay for lesions induced in a region of mitochondrial DNA after a 4 h treatment of CEM cells with bizelesin. Remaining amplification (●, left axes) represents averaged values of the signal for the amplified PCR product, normalized to the amplification of control DNA, from five independent experiments (±SE, where they exceeded marker size). The frequencies of drug-induced region-specific lesions (○, right axes) were estimated using a Poisson distribution. For details see Figure 2 and Materials and Methods. (B) Frequency of bizelesin lesions in bulk DNA (■), mitochondrial DNA (+), and ApoB MAR (○) replotted on the same scale from Figures 6, 7A, and 4, respectively.

weaker ($r = 0.902$, data not shown), than that for the cross-linking motif only (Figure 8). On the other hand, markedly weaker correlation was found when the frequencies of region-specific lesions were plotted against the percentage of A/T in individual regions ($r = 0.6$, data not shown). These results demonstrate that, despite occasional drug binding to other sequences, the cross-linking motif $T(A/T)_4A$ predicts well the relative vulnerability of various regions to bizelesin.

Analogous results for the regions also analyzed for adozelesin illustrate that the regional density of either the more or the less stringent motifs for adozelesin, $5'(A/T)_4A3'$ or $5'(A/T)_3A3'$, respectively, would predict the markedly higher frequencies of adozelesin lesions over bizelesin lesions. Although the less extensive data for adozelesin than for bizelesin prevent a clear-cut conclusion, it seems that, in contrast to bizelesin, adozelesin might be able to induce substantial damage in regions low in either $5'(A/T)_4A3'$ or $5'(A/T)_4A3'$, reflecting lower actual stringency of adozelesin binding.

Drug Cytotoxicity in CEM Cells. Consistent with previous studies in other systems, both bizelesin and adozelesin showed a remarkably potent antiproliferative effects in human acute lymphoblastic leukemic CEM cells (Figure 9).

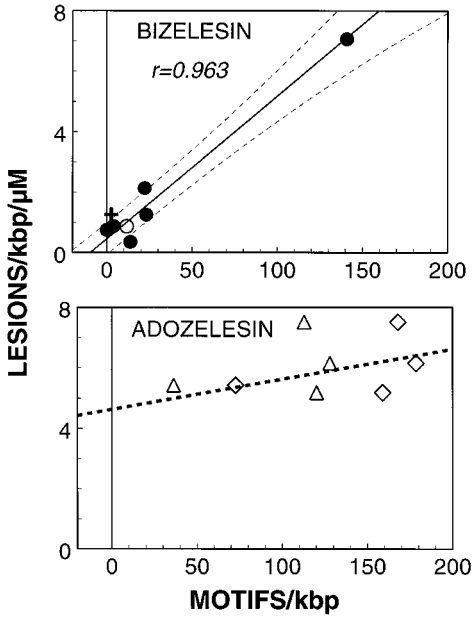

FIGURE 8: Predicted versus actual region-specific DNA lesions in drug-treated CEM cells. Lesions induced by bizelesin (top, ●) and adozelesin (bottom, ◇) in various regions (by QPCR stop assay, Figures 2−4) and bizelesin lesions in bulk genomic DNA (top, ○, by sedimentation analysis, data from Figure 6) are plotted against the density of respective drug binding motifs. Lesions in all regions are normalized per kilobbase pair/micromolar drug by averaging the data corresponding to approximately 20−80% remaining amplification. The motif densities for specific regions, normalized per kbp, are based on analysis of the respective sequences with the $5'T(A/T)_4A3'$ motif for bizelesin (top panel). Bizelesin motif density assigned to bulk DNA was calculated (*33*) with the assumptions of random occurrence of $5'T(A/T)_4A3'$ and DNA composition of 60% AT and 40% GC. Solid and broken lines show, respectively, the linear regression and its 95% confidence limits for bizelesin data ($r = 0.964$). Data for bizelesin lesions in mitochondrial DNA (based on Figure 6A) are plotted (+) but not included in the regression analysis. The bottom panel shows analogous plots for adozelesin, using more and less stringent motifs, $5'(A/T)_4A3'$ (△) and $5'(A/T)_3A3'$ (◇), respectively.

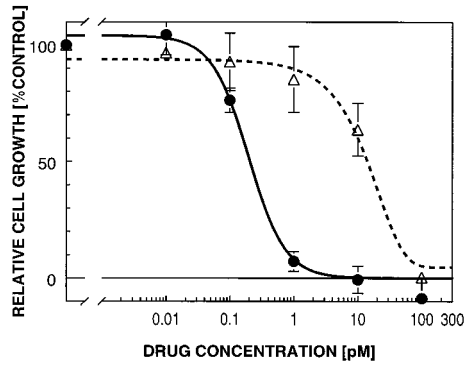

FIGURE 9: Cytotoxicity of bizelesin (●) and adozelesin (△) in CEM cells. Relative growth from 2−4 independent experiments (±SE) was determined on the basis of cell counts after a 48 h incubation with drugs.

Bizelesin, however, was clearly more potent than adozelesin with GI_{50} values (drug concentrations producing 50% net growth inhibition) of 0.19 and 14 pM, respectively. For bizelesin, a similar value (0.6 pM) was determined previously by another assay (*21*). For both drugs, the inhibition curves were rather steep, with GI_{90} values (drug concentrations producing 90% net growth inhibition) of ∼1 and ∼56 pM for bizelesin and adozelesin, respectively.

DISCUSSION

This study focused on the determinants of region-specific damage to cellular DNA in cancer cells by bizelesin and adozelesin, two related AT-specific anticancer minor-groove binding drugs of the CPI family. Bizelesin was found to preferentially target regions containing islands of AT-rich DNA, such as AT-rich MAR domains, with marginal effects on regions poor in its preferred binding motif. Thus, bizelesin effects provide the first-ever documented case of region-specific damage to cellular DNA by a small molecular weight drug.

The relatively small differences in drug binding motifs at the nucleotide level can profoundly affect their region specificity. Adozelesin forms more lesions than bizelesin in various regions including oncogenic and nononcogenic loci (c-*myc* and *HPRT*, respectively). These differences are consistent with the less stringent sequence preferences of adozelesin vs bizelesin ($5'(A/T)_{3-4}A3'$ and $5'T(A/T)_4A3'$, respectively) and the differential abundance of these motifs in the regions examined. Adozelesin tolerance for G/C at the 5′ portions of drug binding sites is corroborated by our preliminary results, where adozelesin but not bizelesin induced damage to telomeric DNA repeats $(GGGTTA)_n$, detected as thermally induced strand breaks with a telomere-specific probe by Southern blotting (Napier and Woynarowski, unpublished data). The compatibility of the adozelesin's minimal consensus motif $(A/T)_2A$ with the telomeric repeats points to a potential utility of adozelesin or similar smaller CPI drugs as telomere-targeting agents, either per se or, ideally, in conjugates with a G/C-recognizing moiety.

The experimentally determined ability of bizelesin to damage several regions of genomic DNA correlates well with the regional density of drug binding motif and markedly better than with overall AT content. Drug-induced lesions are relatively low in regions that are poor in bizelesin binding motif (such as β-globin), and in the bulk of genomic DNA. On the other hand, bizelesin affects islands of AT-rich DNA markedly more than non-AT-rich regions and bulk DNA. The enhanced vulnerability to bizelesin appears to accompany the clusters of $T(A/T)_4A$ sites. Bizelesin preference for such clusters is most obvious with Apo B MAR. Somewhat less profound lesion frequency in the c-*myc* MAR system probably reflects the fact that this PCR system is nearly twice the size of the c-*myc* MAR proper and the flanking sequences have very few potential drug binding sites. Bizelesin's predisposition for AT islands has been recently confirmed in another region identified in GenBank entry Z79699 (*21*). The conclusion that binding motif density reliably predicts relative vulnerability of various regions to drug adduction corroborates and markedly expands our similar observation for low sequence specificity (and non-region-specific) drugs such as cisplatin (*25*).

Bizelesin seems to region-specifically target AT-rich MAR domains in the nucleus. This observation is consistent with the previously noted bizelesin preference for the MAR region in intracellular SV40 DNA (*9*, *10*). Also, preliminary Alu PCR suggests that some regions flanked by Alu repeats, which are highly likely to be "enriched" in AT MAR domains (*32*), are strongly affected by bizelesin. In light of the nonpreferential bizelesin damage to mitochondrial DNA, these results are consistent with damage to nuclear DNA, rather than mitochondrial DNA, as the probable main factor in bizelesin action.

Bizelesin and adozelesin are among the most cytotoxic compounds ever discovered (in the subpicomolar and picomolar range, respectively). This extreme cytotoxicity probably results solely from DNA adducts, as CPI drugs do not react with other cellular macromolecules. Extrapolation of the determined frequency of bizelesin adducts in bulk DNA of CEM cells to drug concentrations corresponding to its GI_{50} and GI_{90} values suggest that bizelesin needs to form only an estimated 1−3 adducts per cell for significant cell growth inhibition. Lesions induced by bizelesin seem to be more lethal than the less localized damage by adozelesin. It remains to be clarified whether this greater lethality reflects an enhanced targeting of AT islands or formation of interstrand cross-links as opposed to adozelesin's monoadducts, or both factors.

AT-rich repetitive sequences, characteristic of many nuclear matrix-associated regions (MARs) (*43*, *44*), may be an important target for anticancer agents. Given their critical role in the organization of nuclear chromatin, targeting of MAR domains is likely to have profound effect on cell function. Lesions in such MARs can be related to the potent antireplicative effect of bizelesin, in which a single drug adduct is sufficient for the inhibition of several genomic replicons (*11*). Single bizelesin hit affects also several SV40 replicons in the process of intracellular SV40 replication (*11*). Another method to analyze replication intermediates confirmed lately that bizelesin inhibits SV40 DNA replication in trans (*45*). The antireplicative effects of bizelesin may be linked to targeting of AT-rich MAR loci. MAR regions are involved in the organization of replicon clusters ("clusterosomes"), which initiate under common control (*46*). MAR propensity for stress-induced unwinding can be pivotal for the function of these loci (*47*). We have postulated recently (*12*) that bizelesin-induced interstrand cross-links can overstabilize AT islands and thus impede their function. It is possible that the consequences of drug-induced structural distortion of a MAR domain may propagate far beyond the directly affected area.

The attention to region-specific DNA targeting as a therapeutically relevant concept has been mainly limited to the idea of inhibiting a target gene with triple-helix-forming oligonucleotides (*48*−*50*). Unfortunately, despite the high specificity of triplex-forming oligonucleotides in cell-free systems, such agents are at most poorly to modestly growth-inhibitory to cultured tumor cells in vitro and have no reported in vivo antitumor activity (*49*−*51*). On the other hand, small molecules can also be rationally designed to recognize divergent motifs with a remarkable specificity at the nucleotide levels (for review see ref *52*). Somewhat surprisingly, however, the understanding of whether and how such agents can target specific domains in cellular DNA remains underdeveloped. Only a few studies attempted to explore the relationship between the various sequence binding motifs at the nucleotide level and the regions of genomic DNA, which can be differentially affected by drugs (*21*, *24*, *53*−*55*).

The reported results with bizelesin and adozelesin, along with the previous studies with tallimustine and cisplatin (*21*, *25*), allow us to generalize the requirements for region-

specific damage in cellular DNA. A substantial specificity at the nucleotide level is an important and necessary but per se insufficient factor. Tallimustine, an AT-specific drug of the distamycin family, is not region-specific, despite the very high sequence specificity at the nucleotide level (*21*). Paradoxically, the highly specific and accordingly infrequent tallimustine sites are distributed throughout the genome nearly randomly. In striking contrast, bizelesin is region-specific because its binding motif is nonrandomly distributed, with clusters in AT islands (*21*, *56*). Moreover, the consequences of DNA lesions in AT islands targeted by bizelesin seem to be dramatically more lethal than non-region-specific lesions by tallimustine and cisplatin (*21*). Thus, targeting critical repetitive sequences (not necessarily coding regions), which allows for clustering of drug binding motif, can be the paradigm for region specificity of small molecular weight agents.

Our findings with bizelesin provide for the first time a proof of principle for this paradigm. Moreover, the preferentially damaged AT-rich islands can be relevant as targets to selectively eradicate tumor but not normal cells. Our recent data suggest that region-specific bizelesin adducts are markedly less lethal to normal than tumor cells (Trevino and Woynarowski, unpublished data). Importantly, bizelesin is not only a potent cytotoxic agent in vitro but also has demonstrated antitumor activity in vivo and its clinical potential is being investigated.

The notion of region specificity can be a relevant, although yet not fully recognized, aspect for other sequence-specific drugs. The confirmed predictive value of in silico analysis of the distribution of drug binding motifs points to sequence analysis, coupled with selective experimental verification of the vulnerability of specific regions to a drug, as a practical approach to explore region specificity of various existing drugs. Further studies in this direction should help to narrow the gap between the substantial progress in the engineering of desired drug binding properties at the nucleotide level (rational drug design) and an emerging area of rational drug targeting.

ACKNOWLEDGMENT

We are grateful to Dr. Maryanne Herzig for many stimulating discussions and helpful suggestions and to Dr. Roza Sypniewska for a critical reading of the manuscript.

REFERENCES

1. Walker, W. L., Kopka, M. L., and Goodsell, D. S. (1997) *Biopolymers 44*, 323−334.
2. Bailly, C., and Chaires, J. B. (1998) *Bioconjugate Chem 9*, 513−38.
3. Cristofanilli, M., Bryan, W. J., Miller, L. L., Chang, A. Y., Gradishar, W. J., Kufe, D. W., and Hortobagyi, G. N. (1998) *Anticancer Drugs 9*, 779−82.
4. Lee, C. S., Pfeifer, G. P., and Gibson, N. W. (1994) *Biochemistry 33*, 6024−30.
5. Weiland, K. L., and Dooley, T. P. (1991) *Biochemistry*, 7559−7565.
6. Bubley, G. J., Ogata, G. K., Dupuis, N. P., and Teicher, B. A. (1994) *Cancer Res. 54*, 6325−9.
7. Lee, M., Roldan, M. C., Haskell, M. K., McAdam, S. R., and Hartley, J. A. (1994) *J. Med. Chem. 37*, 1208−13.
8. Sun, D., and Hurley, L. H. (1993) *J. Am. Chem. Soc. 115*, 5925−5933.
9. Woynarowski, J. M., McHugh, M., Gawron, L. S., and Beerman T. A. (1995) *Biochemistry 34*, 13042−13050.
10. Woynarowski, J. M., Chapman, W. G., Napier, C., and Herzig, M. C. S. (1999) *Biochim. Biophys. Acta 1444*, 201−217.
11. Woynarowski, J. M., and Beerman, T. A. (1997) *Biochim. Biophys. Acta 1353*, 50−60.
12. Woynarowski, J. M., Chapman, W. G., Napier, C., and Herzig, M. C. (1999) *Biochim. Biophys. Acta 1444*, 201−17.
13. McHugh, M. M., Woynarowski, J. M., Mitchell, M. A., Gawron, L. S., Weiland, K. L., and Beerman, T. A. (1994) *Biochemistry 33*, 9158−68.
14. Wanka, F. (1995) *Acta Biochim. Pol. 42*, 127−31.
15. Dijkwel, P. A., and Hamlin, J. L. (1995) *Int. Rev. Cytol. 162A*, 455−84.
16. Boulikas, T. (1995) *Int. Rev. Cytol. 162A*, 279−388.
17. Benham, C., Kohwi-Shigematsu, T., and Bode, J. (1997) *J. Mol. Biol. 274*, 181−96.
18. Zsido, T. J., Beerman, T. A., Meegan, R. L., Woynarowski, J. M., and Baker, R. M. (1992) *Biochem. Pharmacol. 43*, 1817−22.
19. Lee, C. S., and Gibson, N. W. (1991) *Cancer Res. 51*, 6586−91.
20. Li, L. H., Kelly, R. C., Warpehoski, M. A., McGovren, J. P., Gebhard, I., and DeKoning, T. F. (1991) *Invest. New Drugs 9*, 137−48.
21. Herzig, M. C., Trevino, A. V., Arnett, B., and Woynarowski, J. M. (1999) *Biochemistry 38*, 14045−55.
22. Woynarowski, J. M., Napier, C., Koester, S. K., Chen, S.-F., Troyer, D., Chapman, W., and MacDonald, J. R. (1997) *Biochem. Pharmacol. 54*, 1181−93.
23. Monks, A., Scudiero, D., Skehan, P., Shoemaker, R., Paull, K., Vistica, D., Hose, C., Langley, J., Cronise, P., Vaigro-Wolff, A., et al. (1991) *J. Natl. Cancer Inst. 83*, 757−66.
24. Woynarowski, J. M., Napier, C., and Chapman, W. G. (1997) *Proc. Am. Assoc. Cancer Res. 38*, 228.
25. Woynarowski, J. M., Chapman, W. G., Napier, C., Herzig, M., and Juniewicz, P. (1998) *Mol. Pharmacol. 54*, 770−777.
26. Oshita, F., and Saijo, N. (1994) *Jpn. J. Cancer Res. 85*, 669−73.
27. Oshita, F., Arioka, H., Heike, Y., Shiraishi, J., and Saijo, N. (1995) *Jpn. J. Cancer Res. 86*, 233−238.
28. Sykes, R. C., Lin, D., Hwang, S. J., Framson, P. E., and Chinault, A. C. (1988) *Mol. Gen. Genet. 212*, 301−9.
29. Daoud, S. S., Clements, M. K., and Small, C. L. (1995) *Anti-Cancer Drugs 6*, 405−412.
30. Levy-Wilson, B., and Fortier, C. (1989) *J. Biol. Chem. 264*, 21196−204.
31. Boerwinkle, E., Xiong, W. J., Fourest, E., and Chan, L. (1989) *Proc. Natl. Acad. Sci. U.S.A. 86*, 212−6.
32. Tsongalis, G. J., Coleman, W. B., Smith, G. J., and Kaufman, D. G. (1992) *Cancer Res. 52*, 3807−10.
33. Kramer, J. A., Singh, G. B., and Krawetz, S. A. (1996) *Genomics 33*, 305−308.
34. Zsido, T. J., Woynarowski, J. M., Baker, R. M., Gawron, L. S., and Beerman, T. A. (1991) *Biochemistry 30*, 3733−8.
35. O'Neill, J. P., Rogan, P. K., Cariello, N., and Nicklas, J. A. (1998) *Mutat. Res. 411*, 179−214.
36. McWhinney, C., Waltz, S. E., and Leffak, M. (1995) *DNA Cell Biol. 14*, 565−79.
37. Trivedi, A., Waltz, S. E., Kamath, S., and Leffak, M. (1998) *DNA Cell Biol. 17*, 885−96.
38. Malott, M., and Leffak, M. (1999) *Mol. Cell Biol. 19*, 5685−95.
39. Waltz, S. E., Trivedi, A. A., and Leffak, M. (1996) *Nucleic Acids Res. 24*, 1887−94.
40. Chou, R. H., Churchill, J. R., Flubacher, M. M., Mapstone, D. E., and Jones, J. (1990) *Cancer Res. 50*, 3199−206.
41. Goldman, J., and McGuire, W. A. (1992) *Pediatr. Hematol. Oncol. 9*, 309−16.
42. Kariya, Y., Kato, K., Hayashizaki, Y., Himeno, S., Tarui, S., and Matsubara, K. (1987) *Gene 53*, 1−10.
43. Boulikas, T. (1993) *J. Cell. Biochem. 52*, 14−22.
44. Boulikas, T. (1993) *J. Cell. Biochem. 52*, 23−36.

45. McHugh, M. M., Kuo, S. R., Walsh-O'Beirne, M. H., Liu, J. S., Melendy, T., and Beerman, T. A. (1999) *Biochemistry 38*, 11508−11515.
46. Berezney, R., Mortillaro, M. J., Ma, H., Wei, X., and Samarabandu, J. (1995) *Int. Rev. Cytol. 162A*, 1−65.
47. Bode, J., Kohwi, Y., Dickinson, L., Joh, T., Klehr, D., Mielke, C., and Kohwi-Shigematsu, T. (1992) *Science 255*, 195−7.
48. Helene, C., Thuong, N. T., and Harel-Bellan, A. (1992) *Ann. N.Y. Acad. Sci. 660*, 27−36.
49. Gowers, D. M., and Fox, K. R. (1999) *Nucleic Acids Res. 27*, 1569−77.
50. Neidle, S. (1997) *Anticancer Drug Des. 12*, 433−42.
51. Chubb, J. M., and Hogan, M. E. (1992) *Trends. Biotechnol. 10*, 132−6.
52. Neidle, S. (1997) *Biopolymers 44*, 105−121.
53. Gewirtz, D. A., Orr, M. S., Fornari, F. A., Randolph, J. K., Yalowich, J. C., Ritke, M. K., Povirk, L. F., and Bunch, R. T. (1993) *Cancer Res. 53*, 3547−54.
54. Neidle, S., Puvvada, M. S., and Thurston, D. E. (1994) *Eur. J. Cancer 4*, 567−8.
55. Mattes, W. B., Hartley, J. A., Kohn, K. W., and Matheson, D. W. (1988) *Carcinogenesis 9*, 2065−72.
56. Woynarowski, J. M., Hardies, S. C., Trevino, A., and Arnett, B. (1998) in *10th NCI-EORTC Symposium on New Drugs in Cancer Therapy*, Amsterdam, June 16−19, Abstract 528 Kluwer Academic Publishers: Dordrecht, The Netherlands.

BI000729K